International Journal of
Stem Cell Research & Therapy

Research Article: Open Access

Functionalized Nanoscaffolds to Promote Osteogenic Differentiation in Adipose Derived Human Mesenchymal Stem Cells

Venu Polineni[1], Chi-Shuo Chen[2,3], Wei-Chun Chin[2] and Anand Gadre[1]*

[1]*Stem Cell Instrumentation Foundry, University of California, Merced, USA*

[2]*School of Engineering, University of California, Merced, USA*

[3]*Northwestern University, Chicago, USA*

*Corresponding author: *Anand Gadre, Stem Cell Instrumentation Foundry, University of California, Merced, CA 95343, USA, Tel: 209-658-3879, Fax: 209-228-4424, E-mail: agadre@ucmerced.edu*

Abstract

Biocompatible polymers have been successfully implemented to generate nanofibers for bone tissue engineering. This work focused on generating and functionalizing Poly-l-Lactic-co-Glycolic Acid (PLGA) nanofiber scaffolds in the range of 700 nm using the electrospinning technique. Our specific objective is to design synthetic biodegradable scaffolds comprising electrospun nanofibers that will not only be osteoconductive but also contain porosity for bone cell ingrowth enhanced with Adipose derived human Mesenchymal Stem Cells (AdhMSCs) and a sufficient amount of bioactive ingredient such as Demineralized Bone Matrix (DBM) that would serve as a more conducive framework for cell adhesion, proliferation, and differentiation. Cell-scaffolds and controls were subject to immunohistochemistry and visualized using laser scanning confocal microscopy. Osteocalcin and collagen were expressed the highest in cells grown on PLGA nanofibers but were low in cells grown on PLGA film or cells grown without PLGA. Cell viability data showed that PLGA did not cause any significant cell death, therefore mitigating biocompatibility concerns. Our results demonstrate that the nanoscaffolds support the cell proliferation and differentiation and can be used in osteogenic applications.

Keywords

PLGA, Electrospinning, Nanoscaffolds, AdhMSCs, DBM

Introduction

Bone can spontaneously heal and restore function without significant scarring; however, there are several conditions where this ability is compromised, including critical-sized defects through traumatic injury, osteomyelitis, or bone tumor resections. Healing of bone may also be impaired in much smaller defects, and non-union following fracture occurs in 5-10% of cases [1]. Reconstruction and healing of such problematic bone defects is one of the major goals of current research in the field of orthopedics. Regeneration or implantation of bones is a major focus shared by neurosurgery and orthopedics [2]. Costs associated with treatment of fractures in the US are very high and are rising every year [3]. Structural bone grafting surgeries have been widely used to repair or replace bone defects, using autografts, allografts and synthetic materials with autografts being the most commonly used. Fresh autograft has been the gold standard for repair of large bone defects. Surgical management with autografts is frequently required to treat bone and ligament injuries with as many as 300,000 repairs being performed in the U.S. alone each year [4]. Autograft has the ability to stimulate new bone formation by recruitment of mesenchymal stem cells (MSCs) and growth factors from the host bed (osteoinduction). Autograft can also regenerate itself by production of new bone (osteogenesis). Patient pain, cost and limited supply have been the major drawbacks of using autografting as a treatment measure. Though allografting is abundant as a source, the uncertainty of compatibility and disease transmission has limited its use. Complications of autografts such as reduced harvest site strength and donor-site morbidity have necessitated the development of alternative treatment strategies. Due to these drawbacks, developing scaffolds that mimic the architecture of bone tissue at the nanoscale level is one of the major focuses in this field of tissue engineering.

Scaffolds are often designed for specific applications and are fabricated from a variety of biomaterials such as biopolymers, synthetic polymers, ceramics, or metals. Although scaffolds may be made from different materials, within the realm of musculoskeletal tissue engineering, they should possess some common essential characteristics; these include biocompatibility and certain physical, mechanical, chemical, and structural/architectural properties [5,6]. The nanoscale topography of such scaffold surface likewise is critical for the capacity of osseointegration [7,8]. These features make building a functionalized scaffold that can meet with these requirements a great challenge for bone tissue engineering development. However, it is these features that make polymeric fibers excellent candidates for fabrication of implant surfaces and for controlled periprosthetic drug delivery [9,10]. Such polymer nanofiber based scaffolds offer a way of mimicking the geometry of extracellular matrix (ECM) in the human body, with the capacity to recapitulate cellular microenvironment by incorporating chemical and physical cues of ECM [11] and hence can be used as scaffolding materials to facilitate the tissue morphogenesis [12,13]. Therefore, a scaffold should ideally function as a carrier for
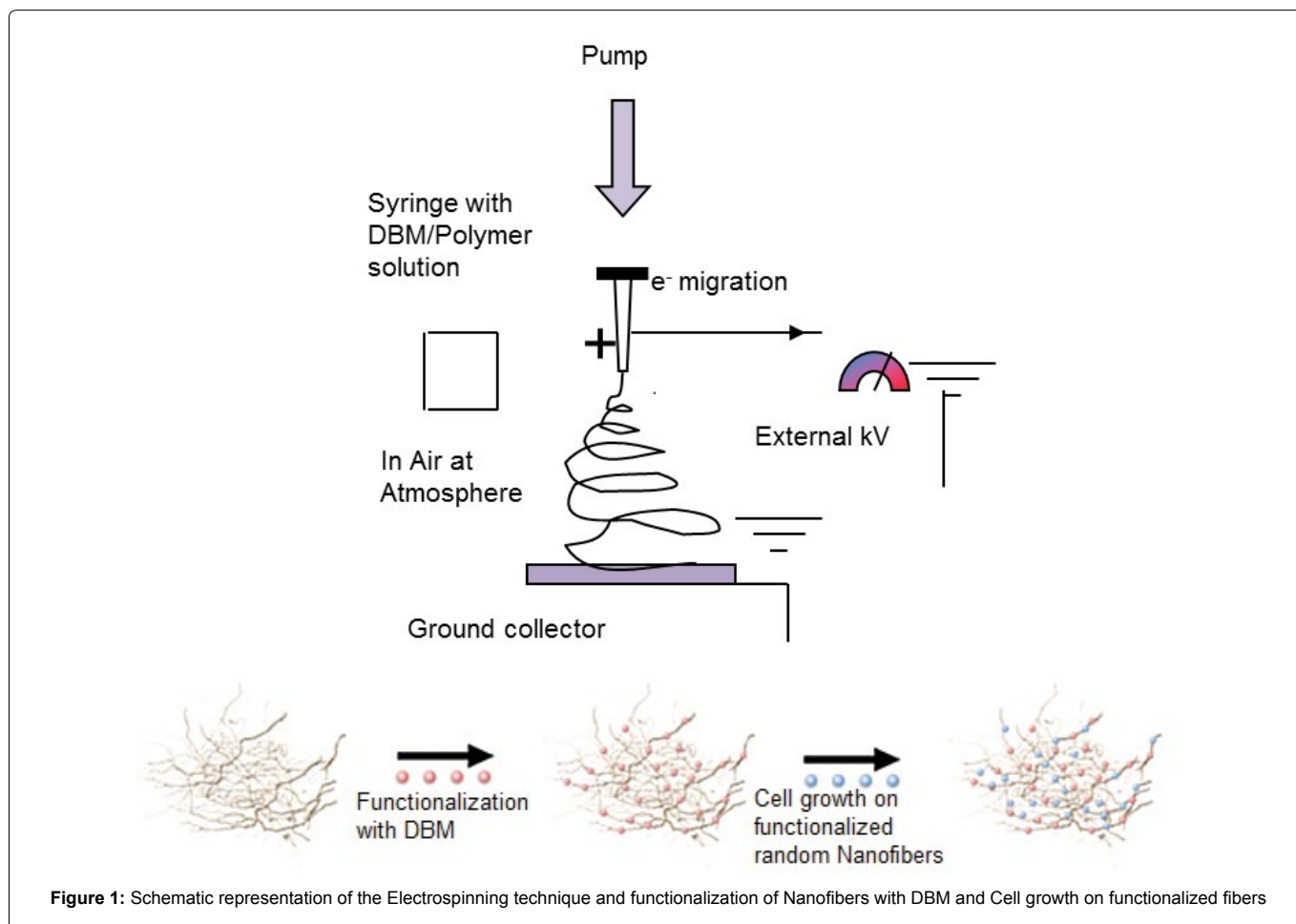
ClinMed
International Library

growth factors as well as cells [14]. To support the latter, a scaffold must be three dimensional and porous, mimicking the ECM produced by healthy bone [15]. Considering this aspect, scaffolds based on nanofibers offer great advantages [15,16] and may serve as a superior scaffold compared to solid-walled architecture for the promotion of osteoblast differentiation and biomineralization [17,18]. Such artificial scaffolds based on synthetic biomaterials can overcome disadvantages of autologous bone grafts, such as limited availability and donor side morbidity. Therefore, in this work we plan to employ the biocompatible and biodegradable polymer PLGA to fabricate functionalized nanofiber scaffolds. By changing spinning parameters, PLGA fibers with diameters ranging from 700 to 1000 nm will be fabricated to mimic extracellular matrix morphology. Demineralized bone matrix (DBM) has been shown to improve the stability of PLGA matrix and also can be potentially used in bone tissue engineering applications [19-21]. Functionalization and testing of scaffolds will be done by incorporating DBM and placing the DBM/nanofiber matrix in vitro to analyze the differentiation and proliferation effects of adding AdhMSCs. This project has the potential to control cell differentiation through scaffold formation that will allow and enhance the growth of tissue and bones, closely mimicking nature in a single-step process. Bone matrix is a morphogenetic substratum that plays a permissive (supportive) role in morphogenesis [22]. DBM utilizes fiber (DBF) technology, which has been proven to be more osteoconductive than DBM particulate because standard particulate DBM is dense and requires more time to break down. Until these dense particles break down, access to natural bone proteins that support and add to healing is limited. Such matrix readily adapts to graft sites and can also be secured with sutures or tacks. DBM has also been proven to be osteoinductive in the athymic rat model and has the most robust osteoinductive response of all the DBM product offerings fibers that is ideal for extraction sites due to its excellent osteoinductivity and osteoconductivity properties and its ability to be placed in extraction site defects [23]. In addition, such matrix displayed a significantly enhanced ability to serve as an osteoconductive graft substitute compared to the particulate form. Such physical matrix or network of entangled bone fibers has exhibited a greater capacity for bone formation than particle-based bone grafting materials. Different surface geometries may impact host cellular interactions as well as diffusion rates of DBM-resident biological molecules. Consequently, some discussion regarding the optimal size and size range of demineralized bone particle suggests that particles less than 250μm are not as osteoinductive as compare to fibrous matrix [24-26]. Many of DBM's proteinaceous components (e.g. growth factors) are known to be potent osteogenic agent and the utilization of DBM provides a degradable matrix facilitating endogenous release of these compounds to the bone wound sites where it is surgically placed to fill bone defects, inducing new bone formation and accelerating healing. The stem cell-based approach proposed in our work provide the advantages of both cellular and molecular therapies for bone regeneration treatments and we believe that the DBM usage would possess essential characteristics such as biocompatibility and specific physical, mechanical, chemical, and structural/architectural properties as well as would enhance functionalized scaffold building that can not only meet requirements for bone tissue engineering, but also help in developing such scaffolds to provide a great opportunity to investigate the impact of microenvironments on the fate of stem cells. By designing biomaterials and such scaffolds that maximally enhance cell attachment, migration, proliferation, and differentiation, we will develop the value of these materials for improving implant fixation, fusion technology needs, and musculoskeletal tissue repair.

Experimental Methods

Materials

Poly (D-lactide-co-glycolide) (PLGA), with a lactic to glycolic acid ratio of 85:15 and a molecular weight of 95,000 Da, and Hexafluoroisopropanol (HFIP), were purchased from Sigma-Aldrich (St. Louis, MO). An automatic syringe pump was purchased from New Era Pump Systems Inc. (Wantagh, NY). 3ml syringes were purchased

Figure 1: Schematic representation of the Electrospinning technique and functionalization of Nanofibers with DBM and Cell growth on functionalized fibers

from Becton, Dickinson and Co. (Franklin Lakes, NJ). Needles with an inner diameter of 0.18mm, 0.22mm, and 0.25mm were purchased from Fisher Scientific. Polytetrafluoroethylene (PTFE) tubing was purchased from VWR International (West Chester, PA). All chemicals were used as supplied without further purification.

Electrospinning set up

PLGA film and fiber scaffolds of PLGA nanofibers were generated by electrospinning using a Design of Experiments (DoE) approach. PLGA dissolved in HFIP was dispensed through a 5-ml syringe via an automatic syringe pump. The needle was suspended vertically over a grounded aluminum collector plate at a fixed distance with an attached voltage supply. The voltage supply was wired to the metal needle via an alligator clip to produce a nonwoven mat of uniform nano- and microscale fibers (Figure 1). All scaffold surfaces were sterilized by UV irradiation for at least 1h, washed and rinse in sterile phosphate buffered saline (PBS), followed by presoaked with cell culture media for 24h.

PLGA-HFIP fibers

PLGA was dissolved in HFIP at a concentration of 10% (w/v) with constant stirring in a glass vial for 12 hours. PLGA-HFIP solution was tested with various flow rates, and optimized results were obtained with 5μL/min flow rate and 0.25mm ID needle. The needle was fixed at a distance of 7cm from the collector plate and was attached directly to a voltage supply and a constant voltage of 15KV was used. 12mm round glass coverslips were pre-cleaned in ethanol and coated with Vectabond (Vector Laboratories, Burlingame, CA), as per manufacturer's protocols, to facilitate adhesion of PLGA. PLGA was then solvent cast using 3% (w/v) PLGA dissolved in HFIP and dried for 1h at room temperature immediately before electrospinning in order to create an adhesive layer between the glass and the fibers. This also served to prevent fiber detachment during cell culture. PLGA fibers were electrospun on top of such film-coated coverslips laid over aluminum foil on a grounded collector plate. Spin coating was used to create these PLGA films to ensure a smooth surface of even thickness. PLGA control films were generated by spin-coating 5% (w/v) PLGA -HFIP solution onto Vectabond-treated glass cover slips for 1 min at 1500 rpm and then placed on a hotplate at 200°C for 30 minutes.

PLGA-DBM-HFIP fibers

DBM was supplied by our collaborator at the Albany Medical College, NY. DBM (200μg) was soaked and stirred for 24h in 3ml of HFIP. The supernatant was mixed in a PLGA-HFIP mixture to obtain a final concentration of 10% PLGA in HFIP. The resulting solution was used to electrospin nanofibers onto the 12mm cover slips creating nanofiber scaffolds. These scaffolds were later seeded with adipose derived human Mesenchymal stem cells (AdhMSCs) (Figure 1).

Adipose derived human Mesenchymal Stem Cell (AdhMSCs) culture

AdhMSCs (STEM PRO®, Invitrogen, CA) were cultured and expanded following the protocols provided by vendor. Briefly, undifferentiated AdhMSCs were expanded using MesenPRO® RS medium (Invitrogen, CA). Experiments were conducted with AdhMSCs at early passage (4-5 passages). Resuspended AdhMSCs were plated on medium presoaked scaffolds and cultured with undifferentiating medium. To differentiate AdhMSCs toward osteoblasts, we cultured AdhMSCs with differentiation medium (STEMPRO®, Osteogenesis Differentiation Kit, Invitrogen). Differentiation medium was changed every 2 days, and cells were cultured on scaffolds for 7 days before executing assay.

Scanning electron microscopy

Scanning Electron Microscope (SEM, Quanta200, FEI machine) was used to characterize various nanofiber matrices. The samples were sputter-coated with 500-Å gold thin film and SEM was performed. We also evaluated the influence of polymer viscosity on electrospun fiber diameters with SEM.

Fluorescence and confocal microscopy

Fluorescence images were obtained using a Nikon TE-2000 microscope, and images were processed using Nikon Elements® software. Laser scanning confocal microscopy was performed using a Nikon Eclipse confocal microscope with images acquired at 20X magnification. Confocal images were processed in NIS Elements® imaging software, and all confocal images within a given experiment were captured using the same laser intensity and gain settings so that intensities could be compared across samples.

Cell viability/proliferation

In order to investigate the biocompatibility of nanofibers, a Live/ Dead® assay (Invitrogen, CA) was applied to investigate the viability of cells after seeding on different substrates for 24 h [27]. Live cells were marked with green-fluorescent calcein, and dead cells were labeled with red-fluorescent ethidium homodimer-1. In addition, we investigated the cell proliferation with a Cell Counting Kit-8 (CCK-8) assay (Dojindo molecular technologies, Gaithersburg, MD) [28]. Hundred microliters of CCK-8 reagent was added to each well containing cells on nanofibers. After about 2 hours incubation, reacted CCK-8 supernatants were transferred to 96-well and the 450 nm absorbance was measured using plate reader.

SYPRO® protein gel analysis for DBM incorporation

In this study, we used SYPRO® (Invitrogen™) protein gel stain to confirm the presence of DBM content within electrospun nanofibers. SYPRO stock reagent was used as purchased and was diluted 1:5000 in 7.5% (v/v) acetic acid solution. 3ml diluted stain solution was poured on nanofiber matrix set in clean dish. After 30 minutes, the nanofiber matrix was washed twice with 7.5% acetic acid solution to remove excess stain (10 minutes per wash).Stained matrix was imaged using a Nikon TE-2000 fluorescence microscope, and images were processed using Nikon Elements® software.

Osteogenic Differentiation

In this protocol, immunohistochemistry was applied to quantify the osteoblast differentiation of hMSCs. Osteocalcin with a ratio of 1:500, (Millipore Co., Billerica, MA, USA) was used as an osteoblast marker to identify differentiated hMSCs [29]. 4', 6'-diamdino-2-phenylindole (DAPI, Invitrogen, 1:3000) staining was used to estimate the cell numbers for normalizing osteocalcin expressing level.

Mineralization assay

Calcium deposition (mineralization) is one of the most significant indications for bone formation. In this study, we used Alizarin Red S (Sigma) to detect mineralization levels [30]. Cells were fixed with 4% paraformaldehyde and rinsed with deionized water (DI water). Alizarin Red S dye was dissolved in DI water (2%wt) and adjusted to a pH of 4.2. Rinsed cells were stained with Alizarin Red S at 20 minutes at room temperature. Excessive dye was removed by DI water wash. Extracellular calcium was stained in orange-red color using Alizarin Red S.

Results and Discussion

Electrospinning to generate a non-woven mat of PLGA fibers

Several parameters were tested to standardize the desirableoperational conditions for the experiments. Once we set up the electrospinning parameters, the fibers can be generated consistently. The parameters we selected for our experiments were 7 cm distance from the needle tip to the collector plate, 5μL/minute polymer flow rate, and 15KV voltage. Cover-slips were first spin coated with Vectabond and were later used for the electrospinning. Scanning electron microscopy images were used to determine the dynamics of the nanofibers obtained by adjusting the viscosity of the polymer solution. PLGA 5% (Figure 2A) and 10% (Figure 2B) solutions were used for electrospinning under specific deposit conditions. Based on the SEM data, the nanofiber diameters were in the range of 600-
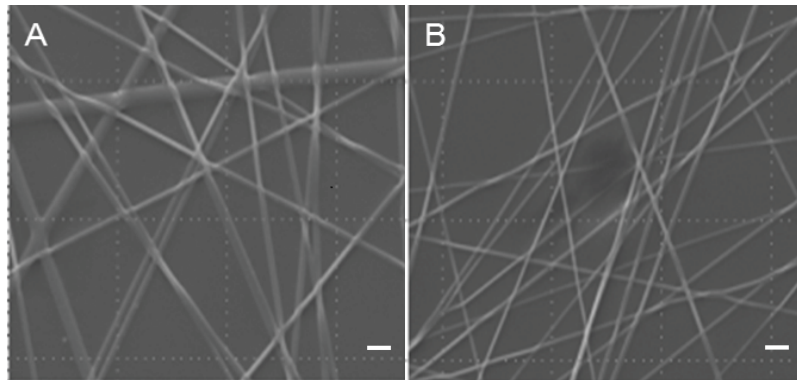
Figure 2: SEM images of NanoscaffoldsA: 5%PLGA nanofibers with a diameter of 1.3μm; B: 10% PLGA nanofibers with a diameter of 679nm; Scale bar=10μm
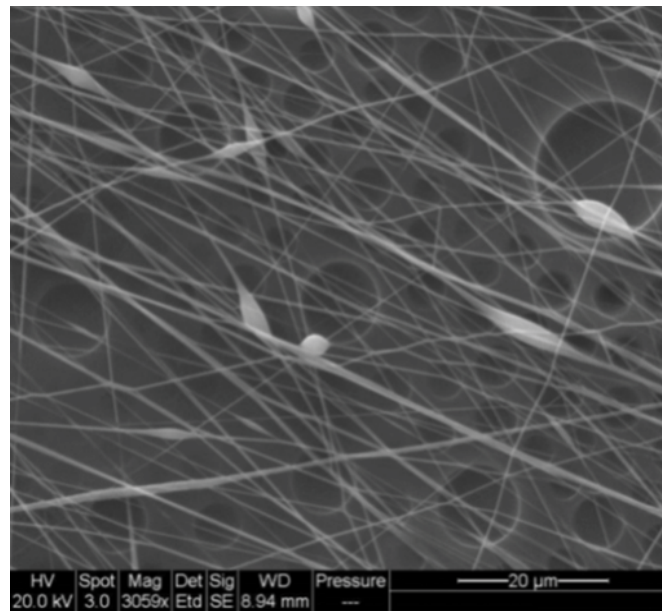

Figure 3: SEM image of functionalized nanofibers; 10% PLGA-DBM nanoscaffolds; Scale bar=20μm
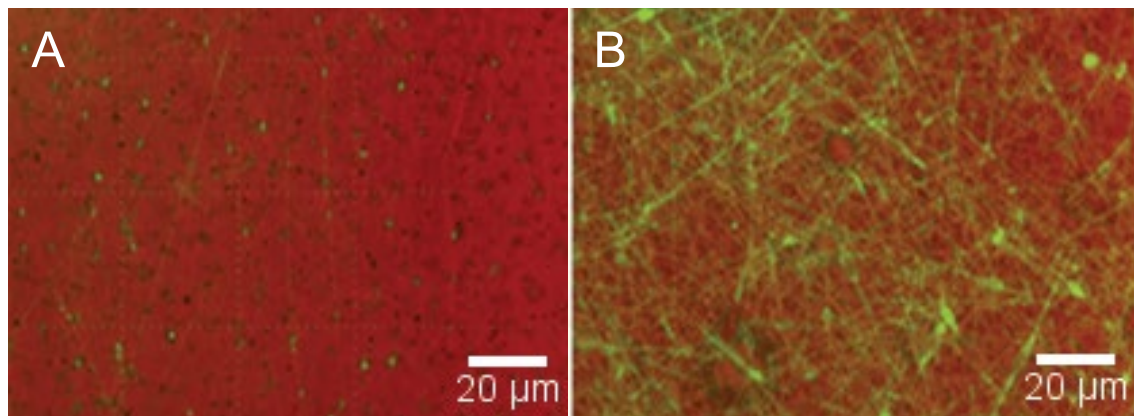

Figure 4: Fluorescent images of functionalized nanofiber matrix. Proteins in nanofibers were labeled with green fluorescent SYPRO® stain. Results indicated higher protein contained in the PLGA-DBM matrix (B), comparing to PLGA matrix (A)

1300 nm with 5% and 10% PLGA respectively. Our results suggest that 10% PLGA fibers were best suited for our experiments and so the subsequent data was obtained using nanofibers obtained from 10%PLGA solution. DBM functionalized nanoscaffolds generated with 10% PLGA were also imaged using the SEM (Figure 3).

Evaluation of the presence of DBM in nanofiber matrix

Our results which include fluorescent images of samples stained with SYPRO® stain confirmed increased protein levels in the matrix treated with DBM. The DBM treated matrix showed a clear green fluorescence when exposed to UV light using an epi-fluorescence microscope (Figure 4).

Evaluation of Cell Proliferation on different nanofibers

Our results showed no obvious viability differences when analyzed after a 24h culture period (n=3) between cells grown on nanofiber and
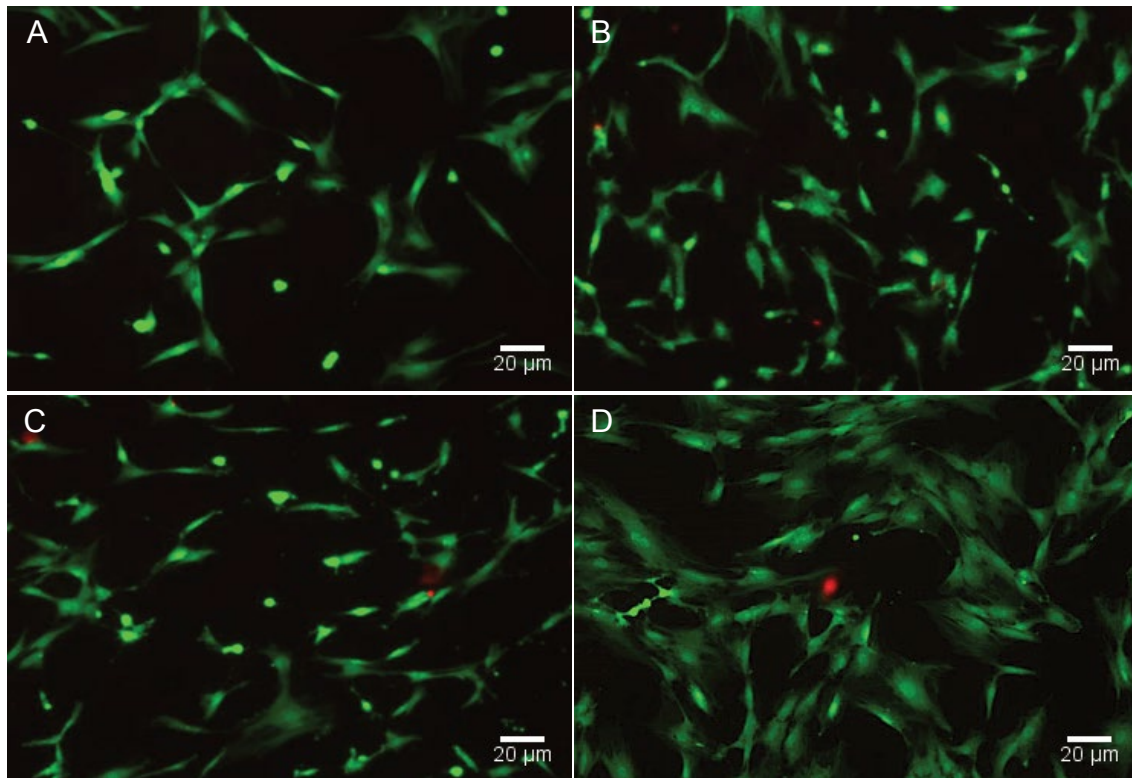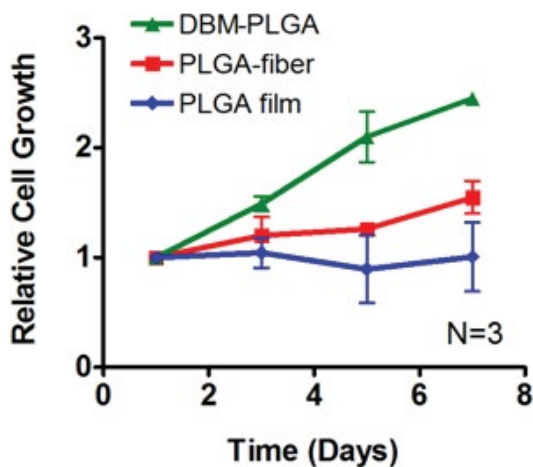
Figure 5: Results of Live/Dead cell assay. Live cells were marked with green-fluorescent calcein, and dead cells were labeled with red-fluorescent ethidium homodimer-1.

A: Cells cultured on PLGA film (Control); B: Cells cultured on PLGA-DBM fibers; C: Cells cultured on PLGA fibers; D: Cells cultured in a petri dish
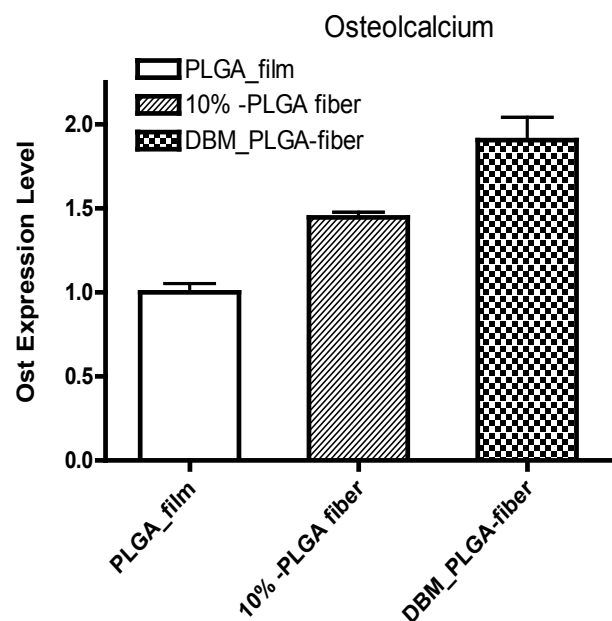

Graph 1: Cell proliferation data obtained over an 8 day period

Graph 2: Osteogenic differentiation data as obtained by Osteocalcium assay (N=3)

the tissue culture dish (Figure 5). Live cells were marked with green-fluorescent calcein, and dead cells were labeled with red-fluorescent ethidium homodimer-1. Compared to the control group (cells grown on PLGA film), there was ~50% increase in proliferation rates in cells grown on PLGA-nanofibers. Moreover, with DBM extraction, hMSCs showed ~100% increase in proliferation on DBM-PLGA-nanofibers (Graph 1).

Osteogenic differentiation

Fluorescence images further established the veracity of the data obtained by SEM. Fluorescent microscopy images of cells subjected to Cal-X and Osteo-R stain, illustrated the differentiation of AdhMSCs into Osteocytes (Figure 6). 6A&D illustrate control samples, 6B&E show cells grown on the nanofibers and 6C&F show cells grown on

DBM characterized Nanofibers. There is a clear indication of cells growing along the fibers and also differentiation in figures 6 B&D when compared to (Figures 6) A&C (n=3). Our results showed that differentiated hMSCs produced ~40% higher Osteocalcin expression on PLGA-nanofiber than cells on PLGA film (Graph 2). This change in differentiation that was observed may be due to the effect of higher surface area of nanofibers as compared to the PLGA films. We hypothesize that controlling the dimension and overall topography of the nanofibers would have significant and positive effects toward
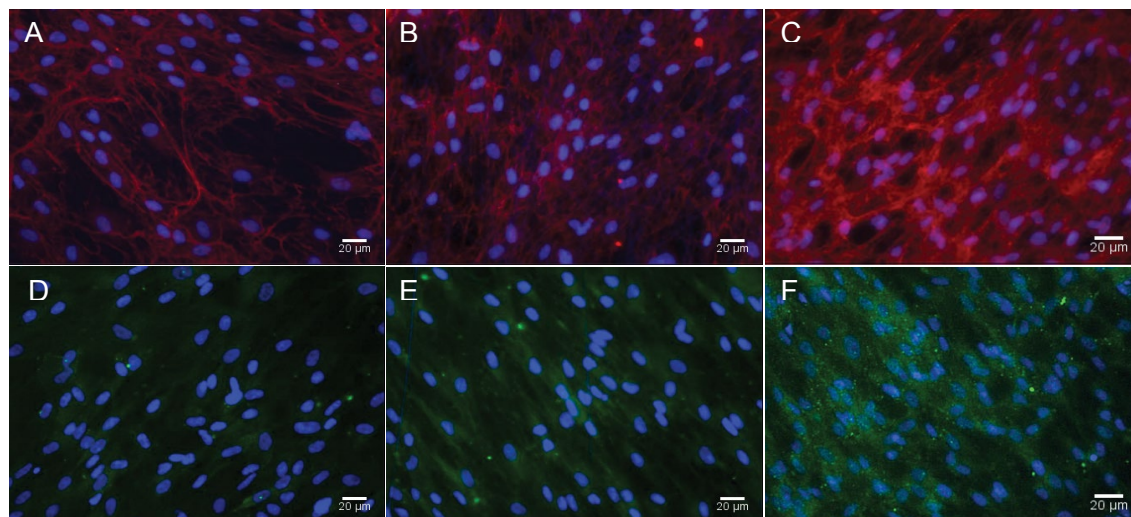
Figure 6: Confocal Microscopy Images of PLGA coated coverslips (A,D); Electrospun PLGA fibers (B,E) seeded with mesenchymal stem cells and Electrospun PLGA-DBM fibers (C,F) A, B & C: Samples subjected to DAPI and Collagen-X stain. D, E & F: Samples subjected to DAPI and Osteocalcin staining
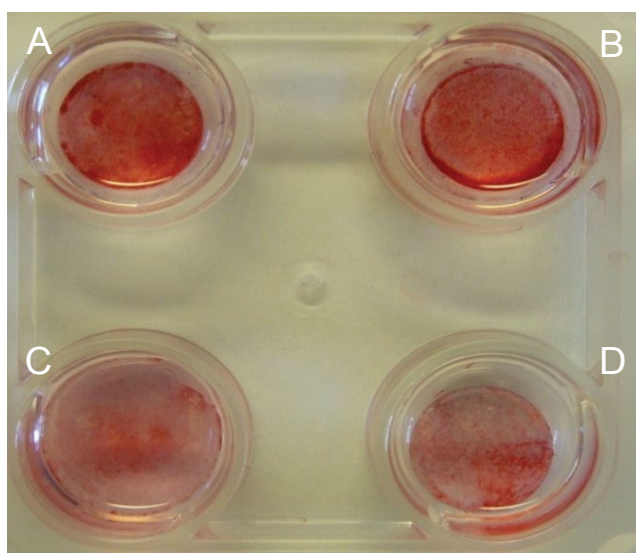

Figure 7: Mineralization assay of differentiated ADhMSCs grown on different nanoscaffolds. Alizarin Red indicates the deposited Calcium, and our results indicated higher mineralization levels in cells grown on PLGA-DBM matrix (B), compared to PLGA matrix (A), PLGA coated coverslip (C) or an uncoated coverslip (D)

cell differentiation as previously demonstrated for other different cell types [31-33]. Moreover, DBM within nanofiber can further stimulate hMSCs with and ~90% higher expression level.

Mineralization assay

Bright orange-red calcium stains were observed, which indicated more mineralized osteoblasts, with differentiated hMSCs on PLGA-nanofibers (Figure 7A) and DBM-PLGA- nanofibers (Figure 7B). In contrast, cells without extracellular calcium deposits showed slightly reddish on the control group (Figure 7C) and spin coated PLGA film (Figure 7D) (n=3).

Conclusions

Here we report the effect of functionalized PLGA nanofibers on adipose derived human mesenchymal cell proliferation and osteogenic differentiation. The nanoscaffold structure supported cell attachment, proliferation, survival and differentiation. ADhMSCs were used in our experiments as a feasible cell source to have them differentiate into osteocytes. The DBM saturation method used in our work supports the osteoconductive properties of the cells. The use

of a biocompatible polymer scaffold and AdhMSCs for generation of osteocytes provides a robust and effective approach for bone regeneration. We anticipate that a more detailed understanding of the interplay of the nanoscaffolds and the cell biology of the AdhMSCs will facilitate the application of the nanofiber-based technology within currently considered tissue engineering techniques; furthermore, lead to the discovery of new therapeutic platforms beyond a narrow focus on autografts with reduced harvest site strength and donor-site morbidity.

References

1. Martin GE, Cockshott ID, Fildes FJT (1977) Fibrillar lining for prosthetic device.

2. Kimelman N, Pelled G, Helm GA, Huard J, Schwarz EM, et al. (2007) Review: gene- and stem cell-based therapeutics for bone regeneration and repair. Tissue Eng 13: 1135-1150.

3. Stevens B, Yang Y, Mohandas A, Stucker B, Nguyen KT (2008) A review of materials, fabrication methods, and strategies used to enhance bone regeneration in engineered bone tissues. J Biomed Mater Res B Appl Biomater 85: 573-582.

4. Martin GE, Cockshott ID, Fildes FJ (1989) Fibrillar product.

5. Laurencin CT, Ambrosio AMA, Borden MD, Cooper Jr JA (1999) Tissue engineering: orthopedic applications. Annual review of biomedical engineering 1: 19-46.

6. Stenoien MD, Drasler WJ, Scott RJ, Jenson ML (1999) Silicone composite vascular graft.

7. Kenawy el-R, Bowlin GL, Mansfield K, Layman J, Simpson DG, et al. (2002) Release of tetracycline hydrochloride from electrospun poly(ethylene-co-vinylacetate), poly(lactic acid), and a blend. J Control Release 81: 57-64.

8. Ramakrishna S, Fujihara K, Teo WE, Lim TC, Ma Z (2005) An introduction to electrospinning and nanofibers.

9. Dersch R, Steinhart M, Boudriot U, Greiner A, Wendorff JH (2005) Nanoprocessing of polymers: applications in medicine, sensors, catalysis, photonics. Polym Adv Technol 16: 276-282.

10. Gerard M, Chaubey A, Malhotra BD (2002) Application of conducting polymers to biosensors. BiosensBioelectron 17: 345-359.

11. Zhao Z, Cusick J, Fowler A, Bhowmick S, Toner M (2003) OPTIMIZATION AND STORAGE OF MICRO-FABRICATED SKIN SUBSTITUTES. in 2003 ASME Summer Bioengineering Conference.

Polineni et al. Int J Stem Cell Res Ther 2014, 1:003

● Page 6 of 7 ●

12. Ko EK, Jeong SI, Rim NG, Lee YM, Shin H, et al. (2008) In vitro osteogenic differentiation of human mesenchymal stem cells and in vivo bone formation in composite nanofiber meshes. Tissue Eng Part A 14: 2105-2119.

13. Wen X, Shi D, Zhang N (2005) Applications of nanotechnology in tissue engineering. Handbook of nanostructured biomaterials and their applications in nanobiotechnology 1: 1-23.

14. Urist MR (1965) Bone: formation by autoinduction. Science 150: 893-899.

15. Fertala A, Han WB, Ko FK (2001) Mapping critical sites in collagen II for rational design of gene-engineered proteins for cell-supporting materials. J Biomed Mater Res 57: 48-58.

16. Pajamäki KJ, Andersson OH, Lindholm TS, Karlsson KH, Yli-Urpo A, et al. (1994) Effect of glass bioactivity on new bone development induced by demineralized bone matrix in a rat extraskeletal site. Arch Orthop Trauma Surg 113: 210-214.

17. Blum B, Moseley J, Miller L, Richelsoph K, Haggard W (2004) Measurement of bone morphogenetic proteins and other growth factors in demineralized bone matrix. Orthopedics 27: s161-165.

18. Dong Z, Shuhua Y, Jin L, Weihua X, Cao Y, et al. (2004) Experimental study on allogenic decalcified bone matrix as carrier for bone tissue engineering. Journal of Huazhong University of Science and Technology [Medical Sciences] 24: 147-150.

19. Damien CJ, Parsons JR, Prewett AB, Huismans F, Shors EC, et al. (1995) Effect of demineralized bone matrix on bone growth within a porous HA material: a histologic and histometric study. J BiomaterAppl 9: 275-288.

20. Champa Jayasuriya A, Ebraheim NA (2009) Evaluation of bone matrix and demineralized bone matrix incorporated PLGA matrices for bone repair. J Mater Sci Mater Med 20: 1637-1644.

21. Schwartz Z, Doukarsky-Marx T, Nasatzky E, Goultschin J, Ranly DM, et al. (2008) Differential effects of bone graft substitutes on regeneration of bone marrow. Clin Oral Implants Res 19: 1233-1245.

22. Urist MR (1997) Bone morphogenetic protein: the molecularization of skeletal system development. J Bone Miner Res 12: 343-346.

23. Gruskin E, Doll BA, Futrell FW, Schmitz JP, Hollinger JO (2012) Demineralized bone matrix in bone repair: history and use. Adv Drug Deliv Rev 64: 1063-1077.

24. Hollinger JO, Mark DE, Goco P, Quigley N, Desverreaux RW, et al. (1991) A comparison of four particulate bone derivatives. ClinOrthopRelatRes : 255-263.

25. Schouten CC, Hartman EH, Spauwen PH, Jansen JA (2005) DBM induced ectopic bone formation in the rat: the importance of surface area. J Mater Sci Mater Med 16: 149-152.

26. Zhang M, Powers RM Jr, Wolfinbarger L Jr (1997) A quantitative assessment of osteoinductivity of human demineralized bone matrix. J Periodontol 68: 1076-1084.

27. Bhattarai N, Edmondson D, Veiseh O, Matsen FA, Zhang M (2005) Electrospun chitosan-based nanofibers and their cellular compatibility. Biomaterials 26: 6176-6184.

28. Zhu Y, Liu T, Song K, Fan X, Ma X, et al. (2008) Adipose-derived stem cell: a better stem cell than BMSC. Cell BiochemFunct 26: 664-675.

29. Fraser JK, Wulur I, Alfonso Z, Hedrick MH (2006) Fat tissue: an underappreciated source of stem cells for biotechnology. Trends Biotechnol 24: 150-154.

30. Bunnell BA, Flaat M, Gagliardi C, Patel B, Ripoll C (2008) Adipose-derived stem cells: isolation, expansion and differentiation. Methods 45: 115-120.

31. Baker BM, Nathan AS, Gee AO, Mauck RL (2010) The influence of an aligned nanofibrous topography on human mesenchymal stem cell fibrochondrogenesis. Biomaterials 31: 6190-6200.

32. Oh S, Brammer KS, Li YS, Teng D, Engler AJ, et al. (2009) Stem cell fate dictated solely by altered nanotube dimension. ProcNatlAcadSci U S A 106: 2130-2135.

33. Teo BK, Ankam S, Chan LY, Yim EK (2010) Nanotopography/mechanical induction of stem-cell differentiation. Methods Cell Biol 98: 241-294.

Polineni et al. Int J Stem Cell Res Ther 2014, 1:003

• Page 7 of 7 •